Evaluation of Mechanical Torque Acting on Scatterer in Microwave Vortex Fields

Evaluation of Mechanical Torque Acting on Scatterer in Microwave Vortex Fields

Hideki Kawaguchi, *Member*, *IEEE*, Hiroaki Nakamura

***Abstract*—This paper discusses generation of vortex fields in microwave frequency range using a corrugated waveguide and a dielectric plate which has spiral structure. Quantitative investigation of the microwave vortex field are carried out by numerical simulations of the Finite Difference Time Domain (FDTD) method. In addition, mechanical torque acting on a scatterer in the microwave vortex field is evaluated aiming an application to remote manipulation of macroscopic objects.**

***Index Terms*—FDTD method, Numerical simulation, Optical vortex, Orbital angular momentum, Mechanical torque, Microwave, Millimeter wave**

I. Introduction

Since a concept of an optical vortex was introduced as the higher azimuthal harmonics of the Laguerre-Gaussian laser fields [1], the optical vortex has been investigated actively not only to understand its fundamental properties but also to be used for various applications. Based on orthogonality in the azimuthal harmonics, it has been attempted that the optical vortex was used for large capacity optical fiber communication [2]. In addition to its particular field distribution and phase structure, it was also pointed out that the optical vortex carries well-defined orbital angular momentum (OAM), and this property was applied to be an optical tweezer [3]. Other possibilities of the vortex fields except for the optical frequency range have been also discussed actively. It was shown that synchrotron radiation from a helical undulator or a circularly rotating electron possess the properties of the vortex field and carries the well-defined OAM [4], [5]. It was proven theoretically that a γ-ray, which was created by Compton's scattering, had the vortex property [6]. It was also investigated to generate the vortex field in microwave frequency range [7]. In particular, a torque acting on a circular ring by the microwave vortex field is evaluated experimentally.

In this work, we first discuss a method of generation of the microwave vortex field using a corrugated waveguide and a dielectric plate which has spiral structure. Then, mechanical torque acting on a scatterer in the microwave vortex fields is evaluated quantitatively aiming remote manipulation of a macroscopic object. The microwave fields has centimeter order wavelength and there exist various kinds of high-power generators already, therefore it is expected that strong torque is created by the microwave vortex field compared with those of the optical or higher frequency range. The microwave vortex fields are investigated by a numerical simulations of the Finite-Difference Time-Domain (FDTD) method since the wavelength of the microwave is comparable size with those of the waveguide or the scatterer in which a para-axial approximation, ray-approximation and a plane wave approximation cannot be employed.

Manuscript received March, 01, 2019. This work was supported in part by the grant of Joint Research by the National Institute of Natural Sciences (NINS). (NINS program No, 01111701)

H. Kawaguchi is with the Division of Information and Electronic Engineering, Muroran Institute of Technology, Muroran, 050-8585 Japan (e-mail: kawa@mmm.muroran-it.ac.jp).

H. Nakamura is with the Department of Helical Plasma Research, National Institute of Fusion Science, Toki-city, Gifu, 509-5292 Japan (e-mail: hnakamura@nifs.ac.jp).

II. Generation of Vortex Field by Corrugated Waveguide and Helical Dielectric Plate

The optical vortex can be generated to be converted from a circularly polarized plane wave by using the spiral dielectric plate (Fig.1) [2]. We here apply this concept to generation of the vortex fields in the microwave frequency range. If we assume that the plane wave comes into the flat side surface of the plate, the phase of outgoing wave at the spiral structure side will be continuously connected everywhere even if the dielectric plate has discontinuous structure in the downstream side when the following relations are satisfied,

$$L\sqrt{\varepsilon_r}k - Lk = 2N\pi \quad \text{or} \quad \frac{L}{\lambda}\left(\sqrt{\varepsilon_r} - 1\right) = N \tag{1}$$

where N is an integer, ε_r is the relative permittivity of the spiral plate, λ and k are the microwave wavelength and wavenumber respectively and L is the difference between the thickness of the thickest and thinnest parts of the spiral plate (Fig.1(b)).

Then, it is very important to use the circularly polarized incident plane wave which has very uniform flat phase plane for creating good quality vortex fields behind the spiral

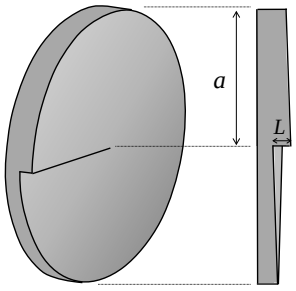

(a) overview (b) side view

Fig. 1. Spiral dielectric plate.

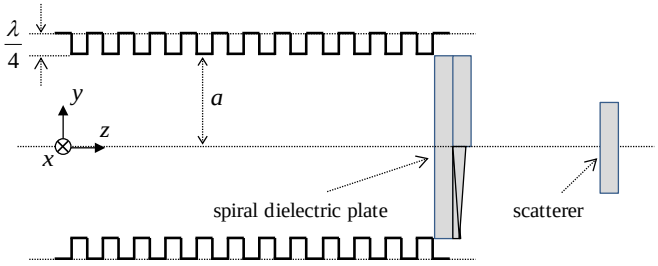

Fig. 2. Cross-section of oversize corrugated waveguide and helical plate.

dielectric plate. It is convenient for such the incident plane wave to use the following HE_{11} mode generated in an oversize corrugated waveguide [8],

(x polarization fields)

$$E_x = -iA\beta\frac{a}{\rho_{01}}J_0\left(\frac{\rho_{01}}{a}r\right),\ E_y = 0,\ E_z = AJ_1\left(\frac{\rho_{01}}{a}r\right)\cos\theta$$

$$H_x = 0,\ H_y = -iA\frac{\omega\varepsilon a}{\rho_{01}}J_0\left(\frac{\rho_{01}}{a}r\right),\ H_z = -A\frac{\beta}{\omega\mu}J_1\left(\frac{\rho_{01}}{a}r\right)\sin\theta \quad (2)$$

where a is the inner radius of the corrugated waveguide, $J_n(x)$ is Bessel's function with n-th order and ρ_{mn} is the m-th zero point of $J_n(x)$. The incident wave for the vortex field is constructed combining (2) and y-direction polarized waves with $\pi/2$ phase difference, which has a characteristics of a circular polarization. The structure of the corrugated waveguide and locations of the spiral dielectric plate and a scatterer are depicted in Fig.2. One of the most important parameters of the corrugated waveguide is a depth of the corrugation at the waveguide inner wall which is taken to be 1/4 wavelength size.

Main purpose of study of the microwave vortex field is creation of strong torque force for objects at a distance. The stress force F_α generated around the scatterer in the microwave vortex field is evaluated by using Maxwell's stress tensor $T_{\alpha\beta}$ on a virtual closed surface S which encloses the scatterer,

$$F_\alpha = \oint_S d\mathbf{f} = \oint_S T_{\alpha\beta}dS_\beta = \oint_S \frac{\partial T_{\alpha\beta}}{\partial x_\beta}dv = \mathbf{F},\ N_\alpha = \oint_S \mathbf{r}\times d\mathbf{f} \quad (3)$$

where α, β denote the coordinate indices x, y, z, $\delta_{\alpha\beta}$ is the Kronecker delta and dS_β and dv are an infinitesimal surface element of S and volume elements inside S respectively.

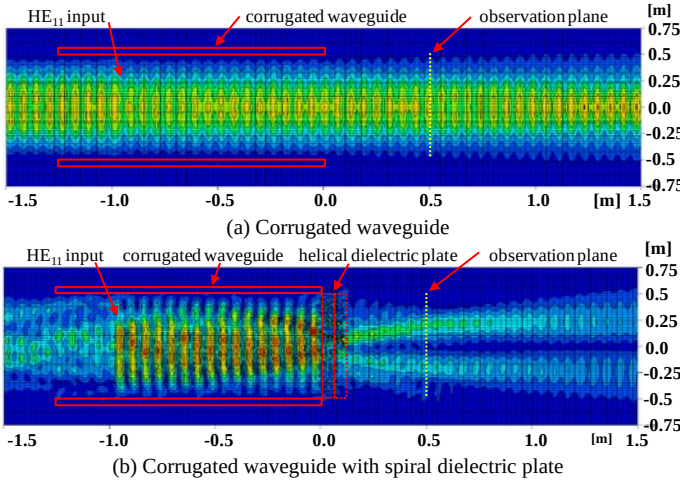

Fig. 3. Distribution of intensity of electric field in y-z vertical cross-section.

III. Numerical Examples

The vortex field of the microwave is investigated by using the 3D FDTD method since the wavelength and the spiral dielectric plate are comparable size each other and any asymptotic analysis such as the ray-approximation and a plane wave approximation cannot be used in this case.

It is assumed that the inner radius a of the corrugated waveguide (see Fig.2) is 50cm and the HE_{11} mode microwave with 1kW power, a frequency f = 2.45 GHz, wavelength λ = 12.2cm, a counterclockwise circularly polarization is excited at an upstream position of the corrugated waveguide. A part of circularly polarized plane wave, which arrives at the spiral dielectric plate on the downstream end of the corrugated waveguide, is converted to the vortex fields as a transmitted wave, and another part of the plane wave will return to upstream direction as a reflected wave. All of the numerical models are discretized by uniform grids of 5 mm, and located inside 300 x 300 x 600 grid space which is surrounded by 8 layers PML absorbing boundary conditions region. All of the time-domain simulations were carried out for over 200 periods to evaluate steady-state of the vortex fields.

A. Evaluation of Vortex Fields

In Fig.3, distributions of intensity of electric field of the microwave in y-z vertical cross-section are depicted. It is shown that the pure and stable HE_{11} mode microwave is emitted from the downstream edge of the waveguide in Fig.3(a) when there is no spiral dielectric plate, and the HE_{11} mode is converted to the vortex fields by the spiral dielectric plate (N = 1, $L = \lambda/2$, ε_r = 9.0 in eq.(1)) in Fig.3(b). It is found from Fig.3 that HE_{11} mode and the vortex fields are stable even in 1 m downstream distance from the corrugated waveguide. In Fig.4, a spontaneous distribution of electric field vectors of the microwave in the x-y vertical cross-section (indicated in Fig.3) are depicted corresponding to Figs.3(a) and (b) respectively. The electric field vectors of the pure HE_{11} mode (Fig.4(a)) has uniform direction, but each vector rotates counterclockwise in time owing to circularly polarization. On the other hand, typical properties of the vortex fields are clearly observed in the Fig.4(b), even if the spiral structure of the dielectric plate has comparable size with the microwave wavelength. There is a phase singular point at the center and the electric field vector rotates by 2π [rad] spatially around the center in the x-y cross-section in addition to in time. It was confirmed that the electric field vectors rotate spatially in opposite direction as that of Fig.4(b) when the HE_{11} mode with a clockwise circularly

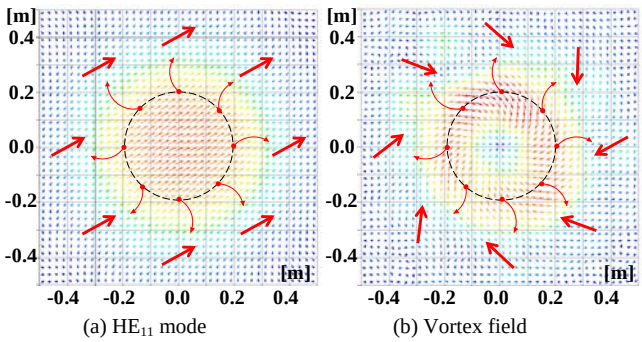

Fig. 4. Electric vector field distribution at x-y vertical cross-section.

TABLE I
Microwave power across spiral dielectric plate

ε_r	L [m]	power [W]
2	2.95 x 10^{-1}	9.63 x 10^{2}
4	1.22 x 10^{-1}	8.33 x 10^{2}
7	7.44 x 10^{-2}	7.25 x 10^{2}
9	6.12 x 10^{-2}	6.70 x 10^{2}
16	4.08 x 10^{-2}	5.15 x 10^{2}

polarization is used. In addition, the electric field vectors rotate by 4π [rad] spatially, that is, the higher order mode vortex field (N = 2) is generated when the dielectric plate with two times longer spiral pitch (N = 2 and $L = \lambda$ in eq.(1)) is used. In Table I, the orbital linear momentum of the vortex fields for various pairs of the relative permittivity ε_r and the spiral pitch L of the spiral plate corresponding to the same vortex field mode N = 1 are given. For example, if we choose a materials of the plate with the higher relative permittivity ε_r , we can select thinner spiral pitch L. It is found that the lower relative permittivity plate can generate higher power vortex fields than those of higher relative permittivity plate.

B. Torque of Vortex Fields

One of predicted applications of the vortex fields in the microwave frequency range is remote manipulation of macroscopic objects. It is well-known that the microwave can create a body force which acts on objects via linear momentum of the microwave fields. The vortex field may create a torque via its orbital angular momentum in addition to the body force. In particular, strong and effective momentum force are expected for the microwave vortex fields by high-power field of order megawatt and wide force distribution of order centimeter. We here evaluate the body force and torque generated by the microwave vortex to calculate Maxwell's stress force acting on the scatterer which is placed in the microwave vortex field (Fig.2). The body force is calculated by eq.(3) and torque $\mathbf{N} = (N_x, N_y, N_z)$ is evaluated on the virtual surface S as a time average value over a period $T = 1/f$ by,

$$N_\alpha = \oint_S \mathbf{r} \times d\mathbf{f}, \quad d\mathbf{f} = T_{\alpha\beta} dS_\beta \tag{4}$$

where $\mathbf{r}$ is the position vector of the infinitesimal area dS_β from the center of the scatterer.

In Fig.5, examples of the scatterers of Fig.2 with 0.5m diameter are depicted. Fig.5(a) is a perfectly electric conductor (P.E.C.) disk with half wavelength thickness, Fig.5(b) is a dielectric disk with half wavelength with ε_r = 9.0 and Fig.5(c) is a dielectric disk which has the same structure but an opposite spiral direction as Fig.1. It is assumed that these scatterers are placed at 0.73 m distance from the downstream end of the corrugated waveguide. In table II, values of each torque components at the steady state for the numerical models of Fig.5 are summarized. Then, x and y components of torque N_x, N_y are created by linear momentum (Poynting vector) of microwave field, so we here focus on N_z component which is created by the angular momentum of vortex fields mainly. To adopt the spiral structure of Fig.5(c), the orbital angular momentum is efficiently took back from the vortex fields as the torque N_z compared with Fig.5(a) and (b). The results in table II are obtained under a lossless condition. Simulation for Fig.5(c) with loss of tan δ = 1.0 x 10^{-3} results in about 4.0% smaller values of the torque, which means such loss will not seriously affect to motion of the scatterer. The absolute value of the torque for Fig.5(c) is still too small to rotate macroscopic objects such as an artificial satellite in space. To roughly estimate a possible maximum case by using a moment of inertia of a simplified disk shape $I = a^2 M/2$ (a : diameter, M : weight), the scatterer of Fig.5(c) with M = 0.1 kg weight can be rotated with angular velocity 3.0 rad/sec after ten minutes illumination of the microwave vortex fields with 1 MW power.

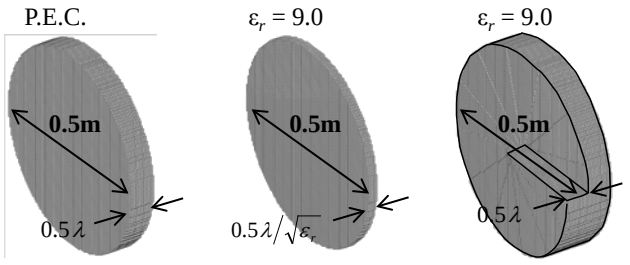

(a) P.E.C. disk (b) dielectric disk (c) spiral structure disk

Fig. 5. Examples of disk scatterers.

IV. Conclusion

In this work, a method of generation of the vortex fields in the microwave frequency region are proposed to use the corrugated waveguide and the spiral dielectric plate. The microwave vortex fields is simulated and evaluated quantitatively by the FDTD method and the torque acting on the scatterer in the vortex fields is also evaluated. For application of the microwave vortex fields to remote manipulation of macroscopic objects, we need to do further investigations such as influences of frequency distribution in microwave and improvements of shape and size of the scatterers for stronger torque.

TABLE II
Steady-state torque acting on scatterer in vortex field

	Fig.5(a)	Fig.5(b)	Fig.5(c)
N_x [N m]	1.3 x 10^{-7}	1.5 x 10^{-9}	2.2 x 10^{-8}
N_y [N m]	8.0 x 10^{-8}	3.1 x 10^{-9}	-1.5 x 10^{-9}
N_z [N m]	1.2 x 10^{-9}	0.94 x 10^{-9}	1.6 x 10^{-8}

References

[1] L. Allen, M.W. Beijersbergen, R.J.C. Spreeuw and J.P. Woerdman, Phys. Rev. A., Vol.45, No.2 (1992), pp.8185-8189.
[2] A.E.Willner, IEEE spectrum, (2016) Aug., pp.34-39.
[3] T. Omatsu, K. Chujo, K. Miyamoto, M. Okida, K. Nakamura, N. Aoki and R. Morita, Opt. Express, 18（2010） 17967—17973.
[4] J. Bahrdt, K. Holldack, P. Kuske, R. Mueller, M. Scheer, and P. Schmid, Phys. Rev. Lett., Vol.111, (2013), 034801.
[5] M. Katoh, M. Fujimoto, H. Kawaguchi, K. Tsuchiya, K. Ohmi, T. Kaneyasu, Y. Taira, M. Hosaka, A. Mochihashi, and Y. Takashima, Phys. Rev. Lett., Vol.118, No.9 (2017), 094801.
[6] Y. Taira and M. Katoh, The Astrophysical Journal, 860:45 (11pp), 2018.
[7] O. Emile, R. Niemiec, C. Brousseau, J. Emile, K. Mahdjoubi, W. Wei, and B. Thide, Eur. Phys. J. D (2016) 70: 172.
[8] K. Ohkubo, S. Kubo, H. Idei, M. Sato, T. Shimozuma, and Y. Takita, Int. Journ. Infrared Millim. Waves, 18, pp. 23-41 (1997).